FERMILAB
AUG 1 1997
LIBRARY

IUCAA -18/97

March 97

Growth of Non-Gaussianity During Cosmological Gravitational Clustering

Fermilab Library
0 1160 0057575 7

By

Varun Sahni

c96/05/25

Invited talk at the second international conference:Astronomy, cosmoparticle physics (Cosmion 96), Moscow, May 25 - June 06, 1996

IUCAA - 18-97

Inter-University Centre for Astronomy and Astrophysics

An Autonomous Institution of the University Grants Commission

Preprint Request (Please quote the preprint number)
email : preprn@iucaa.ernet.in
Fax : 0212-350760
Post : IUCAA, Post Bag 4, Ganeshkhind, Pune 411 007, India

Growth of non-Gaussianity during Cosmological Gravitational Clustering *

Varun Sahni

Inter-University Centre for Astronomy and Astrophysics Post Bag 4, Ganeshkhind, Pune 411 007, India
, IUCAA

ABSTRACT

We discuss the evolution of non-Gaussianity in Cosmological models of structure formation based on gravitational instability. In the quasi-linear regime non-Gaussianity can be characterised by the density moments $S_n = \langle\delta^n\rangle_c/\langle\delta^2\rangle^{n-1}$ which have known analytic forms. During the strongly non-linear regime the formation of caustics leads to growth in non-Gaussianity which can be examined using the Zel'dovich approximation and its perturbative extension: Lagrangian perturbation theory (LPT). We briefly discuss LPT and show that, although the Lagrangian series yields exact quasi-linear moments, it appears to be semi-convergent and therefore of limited overall utility. We follow the evolution of non-Gaussianity in N-body simulations using percolation analysis and the genus curve. We show that the percolation curve is a very sensitive indicator of non-Gaussianity and should be applied to other distributions such as the Cosmic Microwave Background. Examining gravitational clustering using N-body simulations we find that the filling factor of overdense objects decreases with cosmological epoch. The smallness of the filling factor indicates that matter is more likely to be distributed in sheets and filaments (since these occupy less space). We use shape sensitive statistics to study density fields in N-body simulations and find that both filamentarity and pancakeness increase with gravitational clustering: filamentarity being more noticeable, possibly due to the alignement of neighboring clusters in a distribution. Filamentarity also appears to be more pronounced for spectra with greater large scale power, and we expect higher redshift objects in CDM-like models to be noticeably filament-like.

* Invited talk at the Second International Conference: Astronomy, Cosmoparticle Physics (Cosmion 96), Moscow, May 25 - June 6, 1996.

1 NON-GAUSSIANITY IN THE WEAKLY NON-LINEAR REGIME.

The standard paradigm of structure formation based on gravitational instability favours initial (seed) perturbations distributed in the manner of a Gaussian random field. Reasons for this stem both from the central limit theorem and from a consideration of density fluctuations generated by quantum fluctuations in a scalar field during Inflation. The probability density function (PDF) of a Gaussian random field (GRF) has the well known form

$$P(\delta_R) = \frac{1}{\sigma_R(t)\sqrt{2\pi}} \exp\left[-\frac{\delta_R^2}{2\sigma_R^2(t)}\right]. \tag{1}$$

where σ_R is the mean square fluctuation smoothed on a scale R. All odd order moments of a GRF vanish, whereas even orders' can be expressed in terms of σ_R. All connected moments of rank > 2 are zero for such a distribution.

The density field maintains its initial gaussian distribution in the linear regime while $|\delta|, \sigma << 1$. As gravitational instability progresses however, non-linear coupling between the fourier modes δ_k leads to a build up of phase correlations and to the gradual development of a non-Gaussian PDF. In the weakly non-linear regime of gravitational instability the PDF can be described using the Edgeworth expansion (Kendall & Stuart 1977; Bernardeau & Kofman 1995; Juszkiewicz et al. 1993b):

$$\begin{aligned} P(\delta)d\delta &= \frac{1}{(2\pi\sigma^2)^{\frac{1}{2}}} \exp(-\nu^2/2) A(\nu) d\delta, \\ A(\nu) &= \left[1 + \sigma\frac{S_3}{6}H_3(\nu) + \sigma^2\left(\frac{S_4}{24}H_4(\nu) + \frac{S_3^2}{72}H_6(\nu)\right)\right. \\ &+ \sigma^3\left(\frac{S_5}{120}H_5(\nu) + \frac{S_3S_4}{144}H_7(\nu) + \right. \qquad (2) \\ &+ \left.\left.\frac{S_3^3}{1296}H_9(\nu)\right) + ...\right] \qquad (3) \end{aligned}$$

where $\nu = \delta/\sigma$ and $H_n(\nu)$ are the Hermite polynomials

$$H_n(\nu) \equiv (-1)^n \exp(\nu^2/2)\frac{d^n}{d\nu^n}\exp(-\nu^2/2) \tag{4}$$

The non-Gaussian behaviour of the PDF is encoded in $A(\nu)$ which is a function of connected moments of the density field S_n:

$$S_n \simeq \frac{\langle\delta^n\rangle_c}{\langle\delta^2\rangle^{n-1}}. \tag{5}$$

S_3 describes the skewness, S_4 the kurtosis etc., for a Gaussian distribution $S_n = 0$ for $n \geq 3$. The actual values of S_n can be determined in the weakly non-linear (or quasi-linear) regime using a generating function approach introduced by Bernardeau (Bernardeau 1992) [for more details see (Sahni & Coles 1995)]. For scale invariant spectra $P(k) \propto k^n$ with top-hat

final smoothing $S_3 = 34/7 - (n+3)$ (Juszkiewicz et al. 1993a; Bernardeau 1994). Velocity moments have also been studied and have the form (Juszkiewicz et al. 1993a; Bernardeau 1994)

$$\begin{aligned} T_3 &= \frac{\langle\theta^3\rangle}{\langle\theta^2\rangle^2} = -\frac{1}{\Omega^{0.6}}\left[\frac{26}{7} - (n+3)\right] \\ T_4 &= \frac{\langle\theta^4\rangle - 3\langle\theta^2\rangle^2}{\langle\theta^2\rangle^3} \\ &= \frac{1}{\Omega^{1.2}}\left[\frac{12088}{441} - \frac{338}{21}(n+3) + \frac{7}{3}(n+3)^2\right] \end{aligned} \tag{6}$$

(the angular brackets denote an ensemble average). For Gaussian fields, $T_3 = T_4 = 0$. It is interesting that the ratio T_4/T_3^2 is virtually independent of Ω and can therefore be used to probe the value of the primordial spectral index n.

In practice the Edgeworth expansion is only useful for early epochs of gravitational clustering ($\sigma << 1$) before the formation of strongly non-linear objects such as pancakes and other caustics. Further insight into the development of non-Gaussianity in the non-linear regime is provided by the Zel'dovich approximation (Zel'dovich 1970).

2 THE ZEL'DOVICH APPROXIMATION

The Zel'dovich approximation describes a mapping between initial (Lagrangian) coordinates of a particle and final (Eulerian) coordinates. In comoving coordinates it has the form

$$\mathbf{x} = \mathbf{q} + D_+(t)\mathbf{u}(\mathbf{q}) \tag{7}$$

where $D_+(t)$ is the linear growing mode of the density contrast and $\mathbf{u}(\mathbf{q})$ is the initial velocity field of the particle ($\mathbf{u}(\mathbf{q}) = d\mathbf{x}/dD_+$). For irrotational flows $\mathbf{u}(\mathbf{q}) = -\nabla\Phi_0(\mathbf{q})$, where $\Phi_0(\mathbf{q})$ is the linear velocity potential. The Zel'dovich map $\mathbf{q} \rightarrow \mathbf{x}$ can be combined with the requirement of mass conservation $dM = \rho_0\, d^3\mathbf{q} = \rho(\mathbf{x},t)\, d^3\mathbf{x}$, to give a simple expression for the density distribution of matter

$$\begin{aligned} \rho(\mathbf{x},t) &= \frac{\rho_0}{a^3}\left[1 - D_+(t)\lambda_1(\mathbf{q})\right]^{-1}\left[1 - D_+(t)\lambda_2(\mathbf{q})\right]^{-1} \\ &\quad \left[1 - D_+(t)\lambda_3(\mathbf{q})\right]^{-1}. \end{aligned} \tag{8}$$

where λ_1, λ_2 and λ_3 are the eigenvalues of the deformation tensor $d_{ij} \equiv \frac{\partial^2\Phi_0}{\partial q_i \partial q_j}$. (We assume $\lambda_1 > \lambda_2 > \lambda_3$.)

The Zel'dovich approximation predicts the formation of caustics which form when neighbouring particle trajectories intersect [see fig. (1)]. Mathematically the first caustic forms when $1 - D_+(t)\lambda_1 = 0$ ($\lambda_1 > 0$).

Zel'dovich was the first to realise that the network of caustics forms a percolating structure and that the percolating phase occupied a very small physical volume – a characteristic of a strongly non-Gaussian distribution (Zel'dovich 1982). The formation of a network of percolating structures in the Zel'dovich approximation is easy to understand if one notes that caustics form only in regions where $\lambda_1 > 0$ (such regions contract along at least one direction). For a gaussian distribution such regions occupy roughly 92% of the total volume in 3D and therefore percolate in *initial* (Lagrangian) space. [A percolating structure in a Gaussian distribution must occupy > 16% volume in 3D (Shandarin & Zel'dovich 1989).] Since the Zel'dovich approximation preserves topology, a region percolating initially will continue to do so when mapped according to (7). Thus a percolating network of pancakes & filaments forms generically in models of gravitational instability as described by ZA.

Comparing the PDF obtained from ZA with that of N-body simulations (using identical initial conditions) we find quantitatively good agreement at moderately large smoothing lengths. For smaller smoothing scales ZA shows greater departure from N-body predictions (see fig. (2)). Comparisons of ZA with Eulerian perturbation theory (EPT) show that ZA underestimates the quasi-linear moments S_n (Fry 1984; Grinstein & Wise 1987; Munshi et al. 1994).

2.1 Beyond the Zel'dovich approximation – Lagrangian perturbation theory.

An attempt to improve upon the Zel'dovich approximation by including higher order corrections to it was suggested in (Moutarde et al. 1991; Buchert 1989; Buchert 1992; Bouchet et al. 1992).

Such an attempt results in *Lagrangian perturbation theory* (LPT), which contains ZA as its lowest order solution. In a general *Lagrangian* framework

$$\mathbf{x} = \mathbf{q} + \mathbf{\Psi}(t, \mathbf{q}) \tag{9}$$

where $\mathbf{\Psi}$ is treated as an expansion

$$\mathbf{\Psi} = \sum_{i=1}^{n} \mathbf{\Psi}^{(n)} \tag{10}$$

The Lagrangian series (9) & (10) perturbs particle trajectories and complements the Eulerian

Table 1. Quasi-linear moments S_n for lagrangian perturbation series L(n); L(1) is the Zel'dovich approximation.

	Eulerian	L(1)	L(2)	L(3)
S_3	4.857	4	4.857	4.857
S_4	45.89	30.22	44.92	45.89
S_5	656.3	342.2	624.4	654.6
S_6	12653	5200	11666	12568

approach which treats the dimensionless density fluctuation $\delta(\mathbf{x},t) = [\rho(\mathbf{x},t) - \rho_0]/\rho_0$, as an expansion

$$\delta(\mathbf{x},t) = \sum_{n=1}^{\infty} \delta^{(n)}(\mathbf{x},t) = \sum_{i=1}^{\infty} D_+^n(t)\Delta^{(n)}(\mathbf{x}) \tag{11}$$

In analogy with n-th order Eulerian perturbation theory E(n) it was felt that Lagrangian perturbation theory L(n) would provide a consistently closer approach to exact dynamics than L(1) – the Zel'dovich approximation. A comparison of moments in L(n) and E(n) seemed to confirm this impression since L(n) gave accurate results for all quasi-linear moments upto S_{n+1} (Munshi et al. 1994). [See table 1 for a listing of the first four moments for L(1), L(2) and L(3)].

However an important issue which has remained largely unadressed, concerns the domain of convergence of the Lagrangian series (9) & (10). A recently concluded study of LPT in underdense regions led to a surprising result: higher order LPT gave increasingly less accurate results at late times, and the Zel'dovich approximation L(1) outperformed L(2), L(3) etc. in very underdense regions (voids). It now appears that the Lagrangian series L(n) is asymptotic (or semi-convergent) since the inclusion of higher order terms in L(n) beyond an optimal point leads to a reduction in accuracy at late times (Sahni & Shandarin 1996).

3 TOPOLOGICAL MEASURES OF NON-GAUSSIANITY.

As gravitational instability advances into the strongly non-linear regime, matter begins to collect in progressively more overdense structures, the degree of asymmetry between overdense and underdense regions increases and the distribution becomes strongly non-Gaussian. Non-Gaussianity in the strongly non-linear regime can be probed using indicators such as the PDF and its moments described in the last section. However conventional measures of gravitational clustering (PDF, $\xi(r)$ etc.) must be complemented in the strongly non-linear

regime by 'topological' measures such as the genus curve and percolation analysis, which are sensitive to the 'arrangement' of matter on large scales.

3.1 Percolation analysis.

Historically, the use of percolation theory to understand large scale structure was initiated by the Soviet Cosmology school led by Ya.B. Zel'dovich (Zel'dovich 1982; Shandarin 1983; Zel'dovich et al. 1982; Shandarin & Zel'dovich 1983). The methodology one follows in percolation depends upon whether one is studying a set of discrete particles or a continuous density distribution. In this talk I shall mainly deal with density distributions since most discrete distributions can be converted into continuous ones by an appropriate 'smoothing' procedure. Our aim will be to study the connectedness of structure as a function of density threshold in cosmological N-body simulations. Key to our discussion of percolation is the concept of a 'critical density threshold' ρ_c, separating the percolating phase from the unpercolating one. A percolating cluster does not exist in a phase having $\rho > \rho_c$, whereas if $\rho < \rho_c$ *at least one* 'infinite' cluster exists in the system. In practice one deals with finite systems, and we define a percolating cluster to be one which 'runs through' the entire observational sample or simulation box. Varying the density threshold leads to a 'percolation transition' when ρ crosses ρ_c. [Clusters in the above description are defined using a friends-of-friends or 'nearest neighbors' algorithm – we use six nearest neighbors to identify structures.]

A convenient parameter to study percolation is the *filling factor* (FF) defined as the fractional volume in all clusters/voids above/below a density threshold. As the density threshold is decreased from a high initial value, the FF in clusters increases. Eventually the volume fraction in the largest structure grows sufficiently and it fills the entire simulation box, this occurs when $\rho = \rho_c$. For Gaussian random fields the filling factor at percolation is $FF_c \simeq 16\%$, distributions evolving under gravitational instability percolate at higher density thresholds ρ_c and correspondingly lower levels of the filling factor (Klypin & Shandarin 1993; Sathyaprakash et al. 1996; Yess & Shandarin 1996).

It is clear from the above discussion that the percolation threshold ρ_c (equivalently FF_c) is a good measure of non-Gaussianity in a distribution, however it does suffer from some practical limitations, the foremost being its sensitivity to sample geometry. (Since most observational samples are wedge shaped FF_c will depend upon the 'path followed by the percolating cluster' – clearly an undesirable property.) A powerful statistic which does not suffer from these limitations is the volume fraction in the largest cluster v_∞ plotted

as a function of filling factor (or density threshold) (Sathyaprakash et al. 1996; Yess & Shandarin 1996; Sahni et al. 1996). The resulting *percolation curves* can be plotted for both overdense and underdense regions. Fig. (3) shows percolation curves for overdense and underdense regions plotted against the density contrast δ. We show the volume fraction in the largest cluster (thick solid line) and the largest void (thick dashed line). The volume fraction in all clusters/voids *with the exception of the largest* is shown by thin solid/dashed lines. Percolation thresholds for clusters/voids are shown by vertical solid/dashed lines. Error bars showing dispersion computed from four realisations of a given spectrum are typically small. [The models we consider are N-body simulations of scale-invariant spectra $P(k) \equiv \left\langle |\delta_k|^2 \right\rangle \propto k^n$, for $k < k_{Ny}$, and $P(k) = 0$ for $k \geq k_{Ny}$, $n = -2$, -1, 0 and 1, where k_{Ny} is the Nyquist cutoff.]

We find that as clustering progresses the percolation threshold for clusters increases (FF decreases) reflecting the greater ease with which structures percolate. For $n = -2$ the increase in δ_c is monotonic as matter continuously aligns on continuously increasing length scales. However for $n = 0$, δ_c first increases then begins to decrease, as matter collects in small semi-isolated clumps with smaller coherence length (marking the beginning of hierarchical clustering). Thus we find that the percolation threshold δ_c is able to distinguish between complementary scenario's of clustering: long-range filamentarity/pancaking vs. hierarchical clustering.

Percolation curves can also be plotted against the filling factor as is done in figure (4) (left panels). For a Gaussian distribution the two curves will exactly overlap, however for non-Gaussian distributions the asymmetry between the percolating properties of overdense and underdense regions causes the two curves to be shifted with respect to each other and the resulting plot resembles a 'hysteresis curve' (fig. (4)). The area under the hysteresis curve is a good measure of non-Gaussianity, we find that it increases with epoch and is greater for $n = -2$ than for $n = 0$.

From Fig. (3) we find curves showing the volume fraction in all clusters with the exception of the largest peak just before the percolation transition. After percolation the number of disjoint clusters decreases because their mass/volume is transferred to the 'infinite' cluster. The threshold at which the volume fraction in clusters excluding the largest peaks provides an objective threshold at which to identify clusters in a simulation catalogue. We use this method when determining shapes of clusters discussed in Sec. 4.

3.2 Genus curve.

Soon after percolation theory was applied to the analysis of simulations, it was realised that the topology of overdense & underdense regions could also furnish a useful descriptor of large scale clustering [see (Melott 1990) for a review]. The topology of iso-density surfaces lying above/below a density threshold ν can be described by the Genus curve, which is related to the Euler-Poincare invariant, and can be expressed as an integral over the Gaussian curvature K of the surfaces S_ν by the Gauss-Bonnet theorem: $4\pi G(\nu) = \int_{S_\nu} K dA$. (Multiply connected surfaces have $G \geq 0$ while simply connected have $G < 0$.) We note that whereas properties of the *largest cluster* are used to determine PC, *all* clusters lying above/below a given threshold are used to determine GC.

Plotted as a function of the density contrast, GC has a 'bell shape' which is exactly symmetric for Gaussian fields, and has the analytic form $G(\nu) = A(1-\nu^2)\exp(-\nu^2/2)$. During non-linear clustering symmetry between over-dense and underdense regions is broken and the genus curve shows a small shift towards either 'sponge-like' or 'meat-ball-like' topology (Melott 1990). We plot the genus curve as a function of filling factor in fig. (4). When plotted in this manner non-Gaussianity becomes easier to detect because the genus curves for underdense and overdense regions do not exacty overlap (as they do for Gaussian fields). We also find it easier to compare the predictions of the genus and percolation curves with each other (see fig. (4)). For $n = 0$ GC does not appear to distinguish between overdense and underdense regions, however it does show a marked decrease in amplitude presumably caused by nonlinear coupling between modes and increasing phase correlations (Sahni et al. 1996) (also see (Melott 1990)). (This result persists when we compare the genus curve with the 'gaussianised genus' obtained by randomising the phases of particle distributions in N-body simulations.) For $n = -2$ the decrease in amplitude is small but void and cluster curves maintain a roughly constant separation as clustering advances. In general we find the separation between void & cluster curves is very sensitive to the primordial spectral index and shows remarkably little evolution with epoch (Sahni et al. 1996).

Comparing genus and percolation curves for identical initial conditions and at identical Cosmological epochs we find that PC appears to be a more sensitive discriminator of non-Gaussianity than GC (indicated by the area between void and cluster curves in fig. (4)). PC might therefore be used to probe non-Gaussianity in other situations such as for maps of the Cosmic Microwave Background (CMB) (string/texture models of structure formation

predict CMB maps that are significantly non-Gaussian on small angular scales (White et al. 1994)). Some work in this direction is presently in progress (Moessner et al. 1996).

4 FILAMENTS IN ADVANCED GRAVITATIONAL CLUSTERING.

The percolating phase occupies a fractional volume as small as 2-7% in cosmological models such as CDM and CHDM which strongly suggests that the shape of individual objects in such models is more likely to be filamentary or sheet-like since these occupy less space. This assertion can be tested by using statistical measures sensitive to shape such as the 'structure functions' developed by Babul and Starkman (1992) (Babul & Starkman 1992). The structure functions consist of three numbers S_1, S_2 and S_3 each of which takes on values in the range [0,1] and is a function of the radius around a fiducial point which is taken to be the center of mass of the cluster. S_1 characterises filamentarity, S_2 – planarity, and S_3 – sphericity [the reader is referred to (Babul & Starkman 1992; Sathyaprakash et al. 1996) for details]. For our purpose we define density fields on a grid and determine the shape of individual regions lying above a given density contrast. [The density contrast is set at a threshold just higher than δ_c – the critical threshold for percolation. At such thresholds the simulation has lots of unconnected overdense clusters which at slightly lower thresholds link up to form a percolating chain, see fig. (3).]

Our results unambiguously demonstrate that filamentarity dominates over planarity at all epochs and for all cosmological models tested by us. In Fig. 5 we show structure functions averaged over many random but high density points as functions of the window size R. All four epochs of gravitational clustering $k_{\rm NL} = 32, 16, 8$ and 4 (in units of the fundamental mode) are shown in the same panel with darker lines corresponding to later epochs. We find that structures tend to become oblate *only after* a filament-like shape has already developed and that prolateness dominates over oblateness at all epochs for both spectra considered by us. We also find that filamentarity appears to be more pronounced for spectra having greater long range power. We therefore expect to see more filamentary objects at high redshifts in CDM-like models for which clustering of low mass objects took place at higher redshifts when the effective spectral index was $n \leq -2$ (Sathyaprakash et al. 1996; Bond et al. 1996).

5 CONCLUSIONS

We discuss the growth of non-Gaussianity in the quasi-linear and non-linear regimes of gravitational clustering. In the quasi-linear regime non-Gaussianity can be estimated using the moments of the density and velocity fields S_n, T_n and the probability density function (PDF). In the strongly non-linear regime, and until shell crossing, the Zel'dovich approximation and Lagrange perturbation theory (LPT) can be used to probe non-Gaussianity. Although LPT gives exact values for the quasi-linar moments, it does show properties of being an asymptotic (semi-convergent) series and may not be very useful to apply to the late time study of underdense regions (voids). We study the evolution of non-Gaussianity in N-body simulations after shell crossing using topological indicators' such as genus and percolation curves and find both to be very sensitive indicator's of non-Gaussianity. The smallness of the filling factor for clustered objects in N-body simulations indicates that high density regions are more likely to be prolate/oblate since these occupy less space and percolate more easily. We use *shape sensitive statistics* to determine whether pancake or filament-like structures are favoured in N-body simulations. Our results unambiguously demonstrate that overdense systems are more likely to be filament-like thus lending quantitative support to visual impressions (Klypin & Shandarin 1993).

Acknowledgments: Several of the ideas outlined in my talk were results of past and present collaborations with B.S. Sathyaprakash, Sergei Shandarin, Alexei Starobinsky and Dipak Munshi to whom I express my gratitude for numerous discussions and clarifications. My travel to Russia was supported by the Integrated Long term programme of collaboration between India and Russia (ILTP) initiated by the department of Science and Technology (DST), New Delhi.

REFERENCES

Babul A., & Starkman G.D. 1992, *Astrophys. J.*, **401**, 28

Bernardeau F., 1992, *Astrophys. J.*, **392**, 1.

Bernardeau F., 1994, *Astrophys. J.*, **433**, 1.

Bernardeau F. and Kofman, L.A., 1995, *Astrophys. J.*, **443**, 479.

Bond J.R., Kofman L.A. and Pogosyan, D., 1996, Nature, **380**, 603.

Bouchet F.R., Juszkiewicz, R., Colombi S. and Pellat F., 1992, *Astrophys. J.*, **394**, L5.

Bouchet F.R., Colombi, S., Hivon, E., Juszkiewicz R., 1995, *Astron. Astrophys.*, **296**, 575

Buchert T., 1989, *Astron. Astrophys.*, **223**, 9.

Buchert T., 1992 *Mon. Not. R. astr. Soc.*, **254**, 729.

Fry J.N., 1984, *Astrophys. J.*, **279**, 499.

Grinstein B. and Wise M.B., 1987, *Astrophys. J.*, **320**, 448.

Juszkiewicz R., Bouchet F.R. and Colombi S., 1993, *Astrophys. J.*, **412**, L9.

Juszkiewicz R., Weinberg D.H., Amsterdamski P., Chodorowski M. and Bouchet F.R., 1995, *Astrophys. J.*, **442**, 39.

Kendall M. and Stuart A., *The Advanced Theory of Statistics, Volume 1*, (Griffin & Co., London, 1977).

Klypin A.A., & Shandarin S.F. 1993, *Astrophys. J.*, **413**, 48

Kofman L.A., Bertschinger E., Gelb J.M., Nusser A. and Dekel A., 1994, *Astrophys. J.*, **420**, 44.

Melott A.L. 1990, Physics Reports, **193**, 1

Moessner R., Kneiss, R., Sahni, V., Sathyaprakash, B.S., Shandarin, S.F., 1996 (In preparation.)

Moutarde F., Alimi J.M., Bouchet F.R., Pellat R. and Ramani A., 1991, *Astrophys. J.*, **382**, 377.

Munshi D., Sahni, V. & Starobinsky, A.A., 1994, *Astrophys. J.*, **436**, 517.

Sahni V. & Coles, P., 1995, Phys. Rep. **262** (1995) 1.

Sahni V. & Shandarin, S.F., 1996, MNRAS in press.

Sathyaprakash B.S., Sahni V. & Shandarin, S.F., 1996, *Astrophys. J.*, **462**, L5-L8.

Sahni V., B.S. Sathyaprakash & Shandarin, S.F., 1996, *Astrophys. J.* submitted.

Shandarin S.F. 1983, Soviet Astron. Lett., **9**, 104.

Shandarin S.F., & Zel'dovich Ya. B. 1983, Comments Astrophys., **10**, 33.

Shandarin S.F., & Zel'dovich Ya. B., 1989, Rev. Mod. Phys., **61**, 185.

White M., Scott D., & Silk J. 1994, Ann. Rev. Astr. Ap., **32**, 319.

Yess C., & Shandarin S.F. 1996, ApJ, (In press).

Zel'dovich Ya.B., 1970, A&A, **4**, 84.

Zel'dovich Ya. B. 1982, Soviet Astron. Lett., **8**, 102.

Zel'dovich Ya.B., Einasto J. and Shandarin S.F., 1982, *Nature*, **300**, 407.

Figure 1. A two dimensional realisation of the Zel'dovich approximation with random (Gaussian) initial conditions demonstrates the formation of a percolating network of caustics. Reproduced, with permission, from (Sahni & Coles 1995).

Figure 2. Probability density function (PDF) for the lognormal distribution (solid line) and the Zel'dovich approximation (dashed line) is shown for three different smoothing lengths: $R_s = 18, 12, 6h^{-1}$Mpc., corresponding to $\sigma = 0.11, 0.26, 0.55$. Filled regions correspond to the results of N–body simulations of a standard CDM model. Reproduced, with permission, from (Kofman et al. 1994).

Figure 3. Percolation curves are plotted as functions of the density contrast. The thick solid/dashed line corresponds to the filling factor of the largest cluster/void (*ie.* the ratio of the volume in the largest cluster/void to the total volume in clusters/voids). The thin solid/dashed lines show the filling factor of the remaining clusters/voids. The vertical solid/dashed lines correspond to the critical density contrast marking percolation for clusters/voids. The scale of nonlinearity $k_{\rm NL}^{-1}$ (measured in units of the fundamental mode) increases from top to bottom.

Figure 4. Percolation (left panels) and genus curves (right panels) are plotted as functions of the filing factor (FF) for N-body simulations of scale invariant spectra with index (a) $n = 0$ and (b) $n = -2$. The panels illustrating percolation have solid/dashed lines showing the FF in the largest cluster/void as a function of the total FF. The panels illustrating genus have solid/dashed lines showing the genus curve for overdense/underdense regions plotted against the total FF. The vertical solid/dashed lines correspond to the filling factor at percolation for clusters/voids. Reproduced, with permission, from (Sahni et al. 1996).

Figure 5. Structure functions averaged over random (but high density) points are shown as functions of the window radius R (measured in units of the grid size). Curves are for the epochs $k_{\rm NL} = 32, 16, 8$ and 4 (in units of the fundamental mode) with heavier lines corresponding to later epochs. Reproduced, with permission, from (Sathyaprakash et al. 1996).

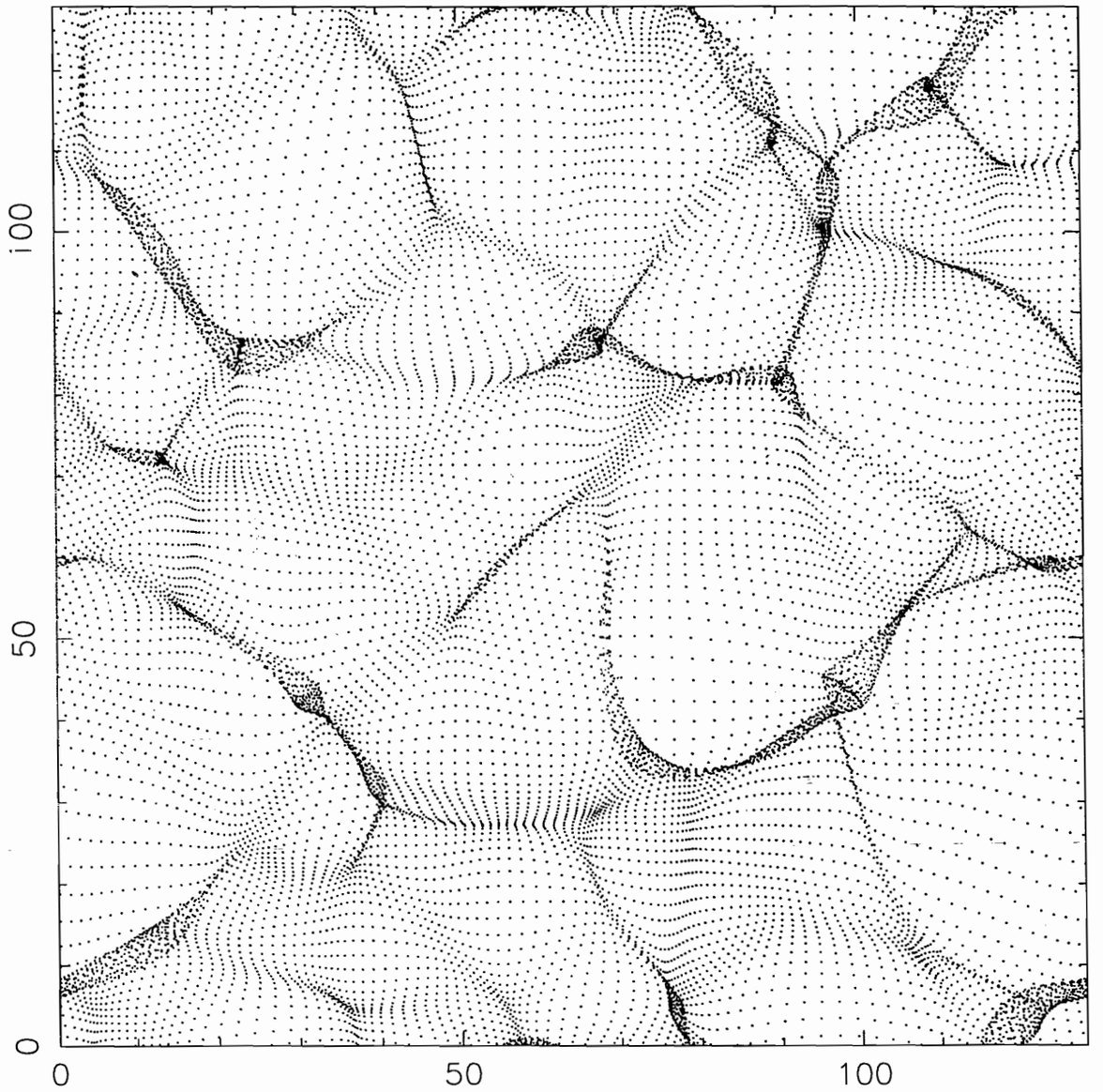

Fig. 7

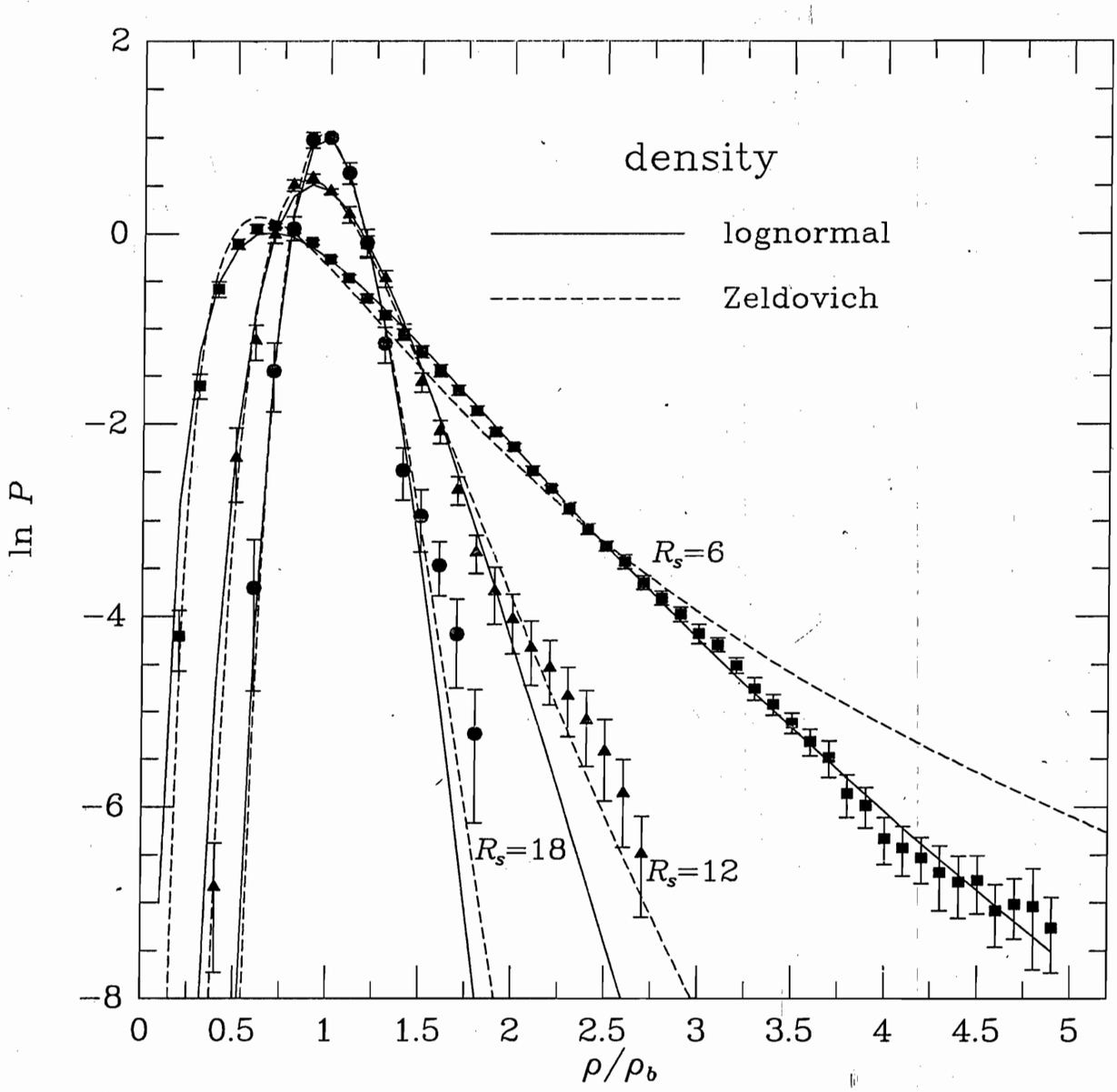
density
lognormal
Zeldovich
R_s=6
R_s=12
R_s=18
ln P
ρ/ρ_b
2
0
−2
−4
−6
−8
0
0.5
1
1.5
2
2.5
3
3.5
4
4.5
5

Fig. 2

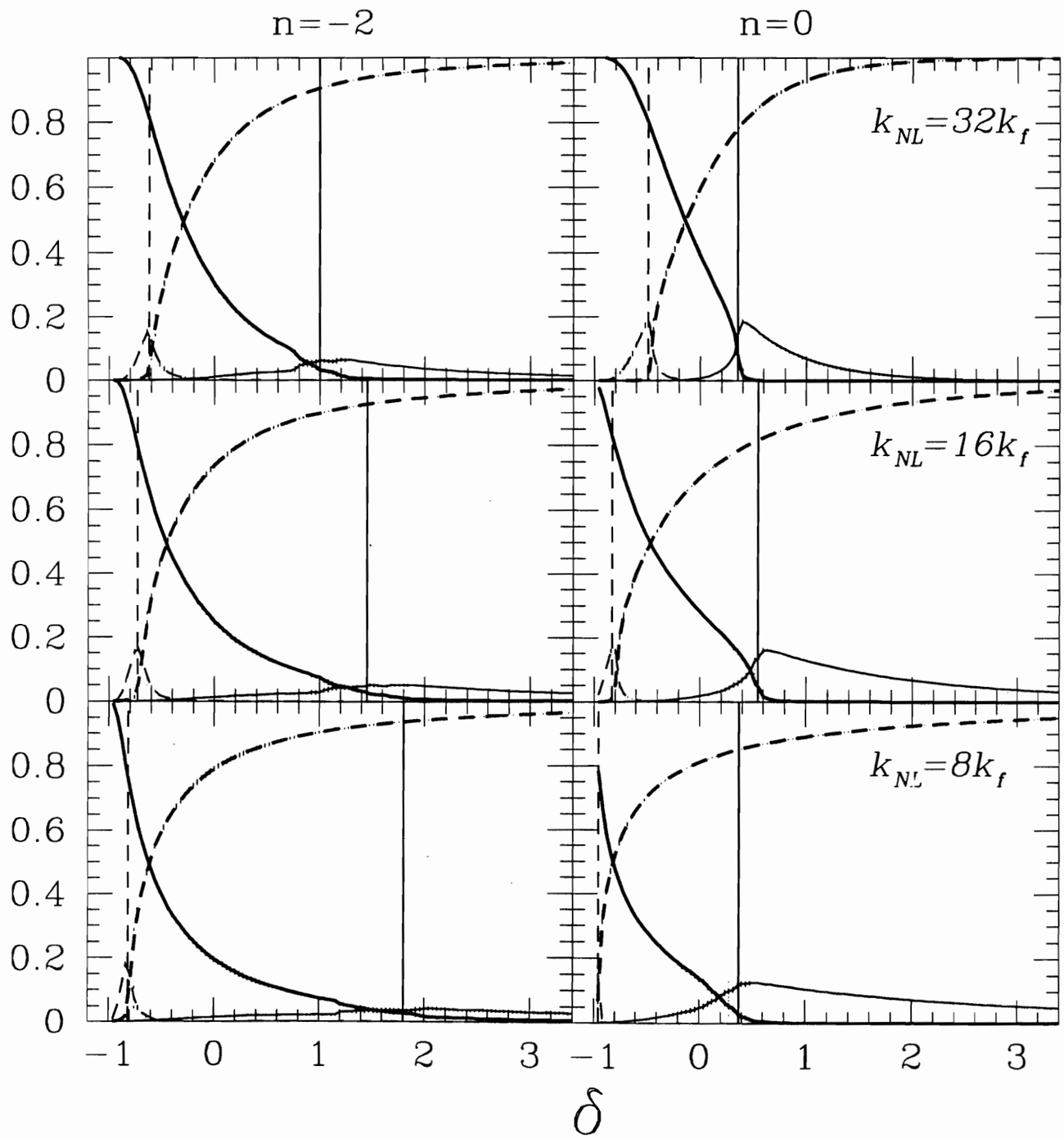

Fig. 3

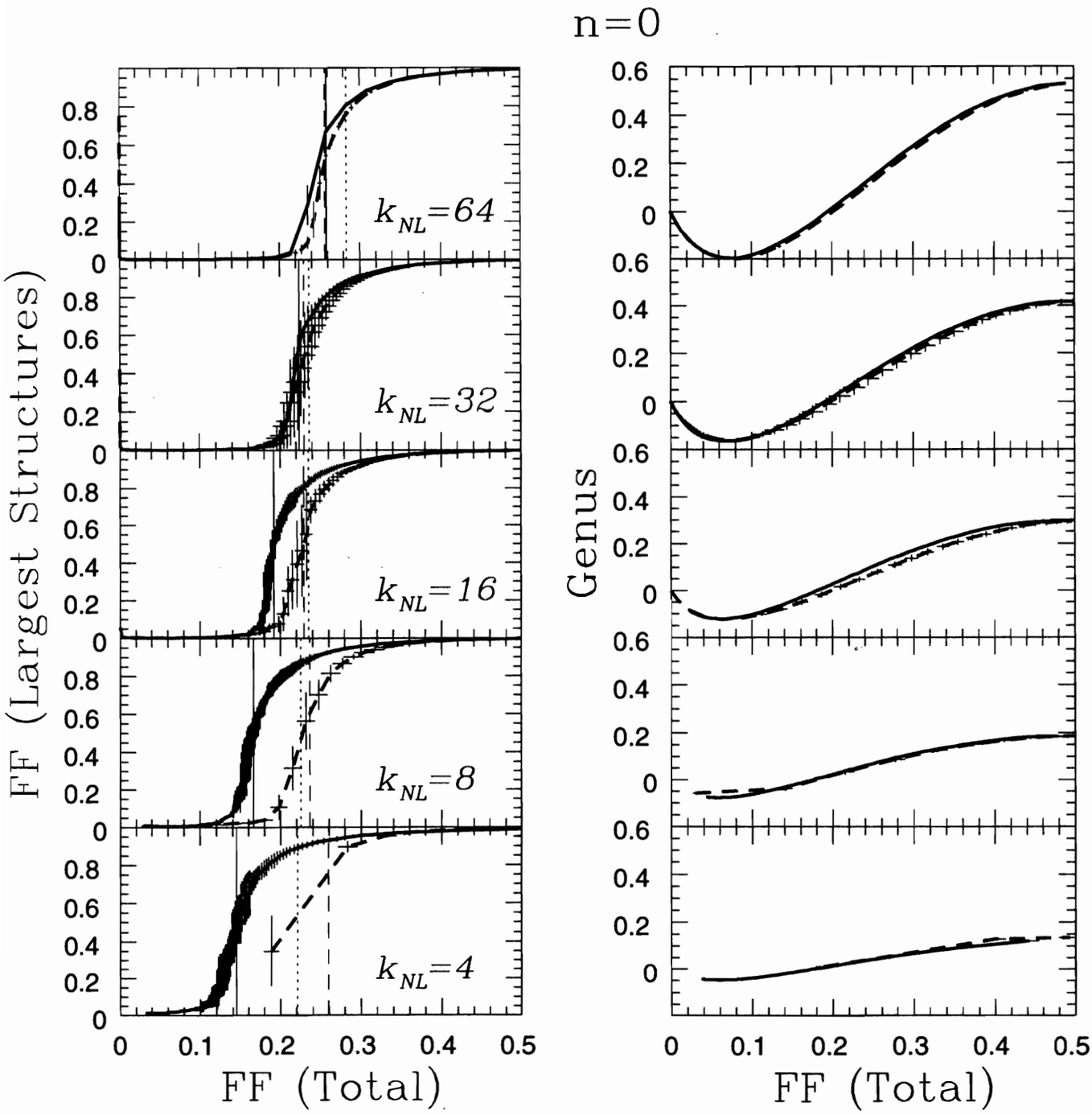
n=0
FF (Largest Structures)
Genus
k_{NL}=64
k_{NL}=32
k_{NL}=16
k_{NL}=8
k_{NL}=4
FF (Total)
FF (Total)

Fig. 5a.

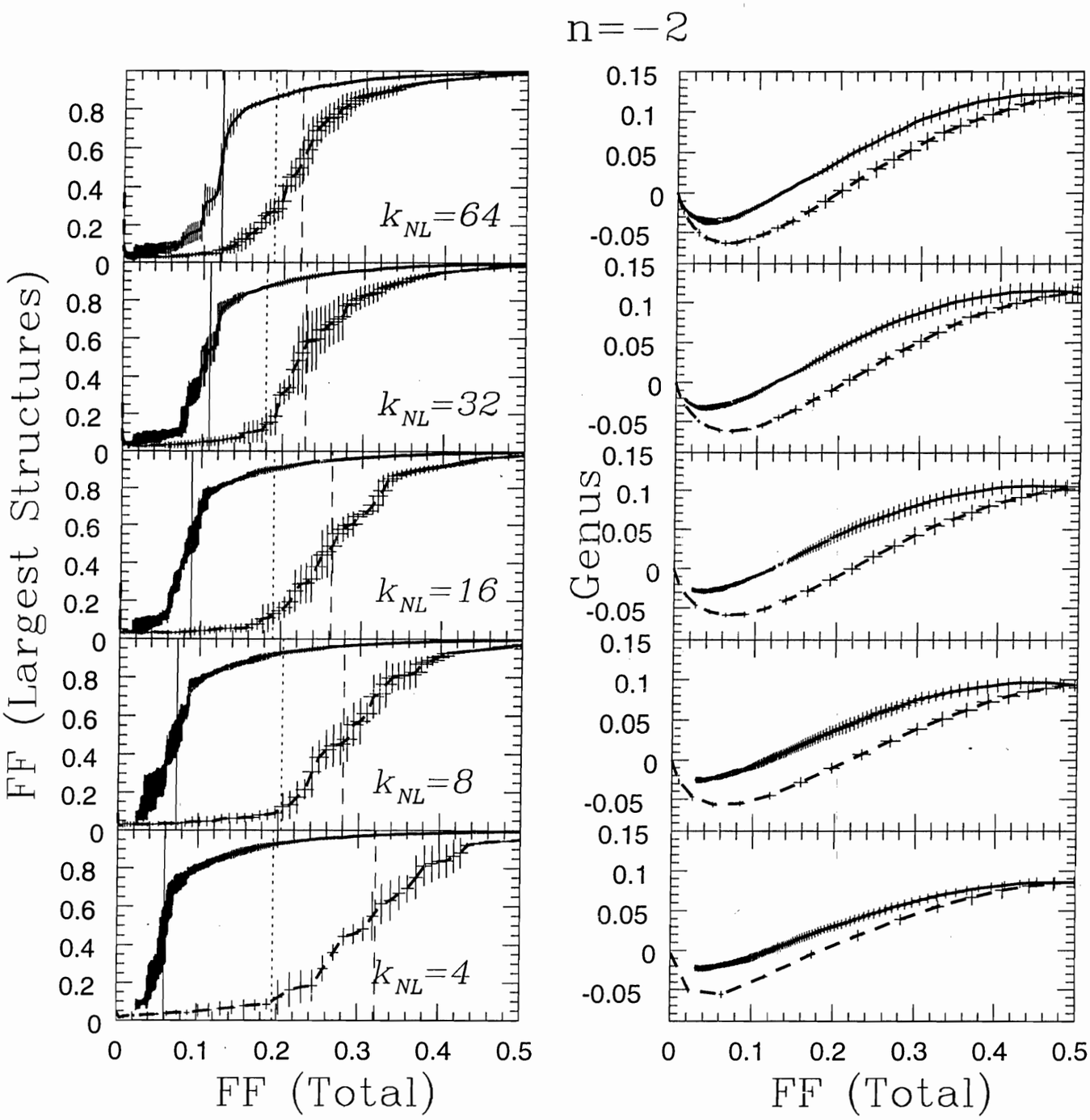
n=−2
FF (Largest Structures)
Genus
k_{NL}=64
k_{NL}=32
k_{NL}=16
k_{NL}=8
k_{NL}=4
FF (Total)
FF (Total)

Fig. 4b

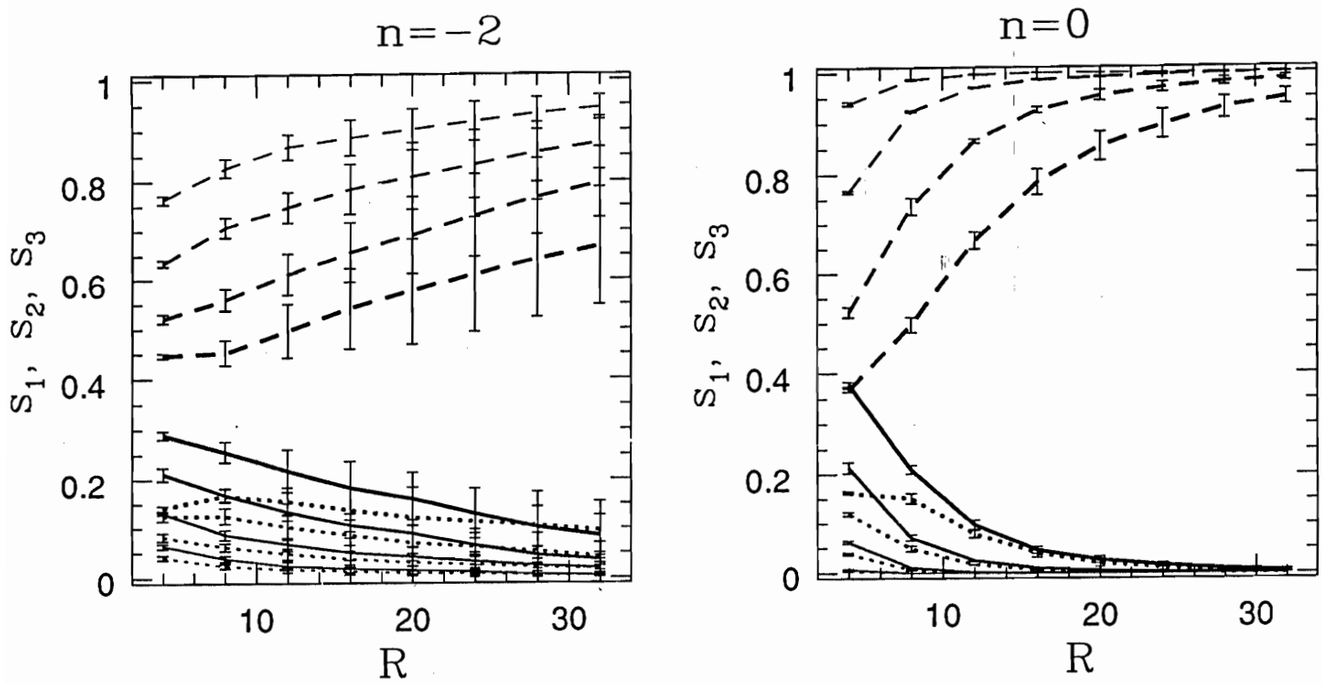

Fig. 5